

Anisotropy and periodicity in the density distribution of electrons in a quantum well

Y. Yayon, M. Rappaport, V. Umansky, and I. Bar-Joseph

Department of Condensed Matter Physics, The Weizmann Institute of Science, Rehovot 76100, Israel

(Received 17 February 2002; published 31 July 2002)

We use low temperature near-field optical spectroscopy to image the electron density distribution in the plane of a high mobility GaAs quantum well. We find that the electrons are not randomly distributed in the plane, but rather form narrow stripes (width smaller than 150 nm) of higher electron density. The stripes are oriented along the $[1\bar{1}0]$ crystal direction, and are arranged in a quasi-periodic structure. We show that elongated structural mounds, which are intrinsic to molecular beam epitaxy, are responsible for the creation of this electron density texture.

DOI: 10.1103/PhysRevB.66.033310

PACS number(s): 73.21.Fg, 71.35.-y, 78.55.Cr, 78.67.De

The two-dimensional electron system (2DES) that is formed in a semiconductor quantum well (QW) is a major platform for studying electron interactions in two dimensions. The electrons in this structure are confined to a thin layer, typically 10–20 nm wide, and are free to move only in the direction parallel to that layer. The significant advance over the last two decades in growth of semiconductor heterostructures by molecular beam epitaxy (MBE), particularly of the GaAs/Al_xGa_{1-x}As material system, has made a critical contribution that facilitated these studies. In addition to achieving high purity and excellent crystalline quality, MBE allows tailoring of the potential and doping profile inside the semiconductor with atomic layer precision. Using modulation doping the 2DES can be spatially separated from the ionized impurities, thus strongly enhancing the electron mobility.¹ Indeed, 2DES samples with high electron mobility, of 10^6 – 10^7 cm²/(V sec), are readily available today and serve for a variety of studies.

Irregularities in the crystal structure, however, are always present and introduce a disorder potential even in these high quality samples. The disorder becomes particularly important and determines the system behavior when it gives rise to spatial fluctuations in the electron density. A particular example is the behavior in high magnetic field, which is governed by the filling factor ν , the ratio between the electron and magnetic flux densities. Clearly, a spatially varying density would translate into spatial fluctuations of ν and lead to inhomogeneous behavior. Nevertheless, despite their importance relatively little is known about the nature of these electron density fluctuations. It was therefore natural that with the evolution of scanning-probe experimental techniques, a considerable effort was directed to resolving spatial inhomogeneities in the system properties.^{2–6} Near-field spectroscopy^{7,8} studies have proven to be particularly useful in that context. The high spatial resolution that can be obtained, typically 100–200 nm, and the wealth of information contained in the optical spectrum made it a favorable technique for studying the local properties of semiconductor QWs.

In this work we use near-field photoluminescence (PL) spectroscopy to study spatial correlations in the distribution of the electron density in a gated 2DES. Our ability to extract the electron distribution from the PL spectrum derives from the fact that a photo-excited electron-hole pair binds to a

“native” electron in the 2DES and creates a bound complex, known as a negatively charged exciton, X^- .^{9,10} The X^- can be easily identified in the PL spectrum as a peak which appears ~ 1 meV below the neutral exciton, X , peak (Fig. 1), and its intensity is directly proportional to the average electron density, n_e . This proportionality is demonstrated in the inset of Fig. 1, which shows the area under the X^- peak (measured in the far field) as a function of n_e . We have recently shown that this proportionality between the intensity and the electron density holds also locally: regions with high electron density give a large X^- signal, and vice versa.^{3,11} This is demonstrated in Fig. 1, which shows two spectra measured at two nearby points in the sample. It is seen that the intensity of the X^- peak is significantly different between the two locations while the X peak is nearly the same. Thus integrating the area under the X^- peak at each point (shaded area in Fig. 1) yields a value which is proportional to the local electron density, $I_{X^-}(x,y)$. Hence, by photo-exciting

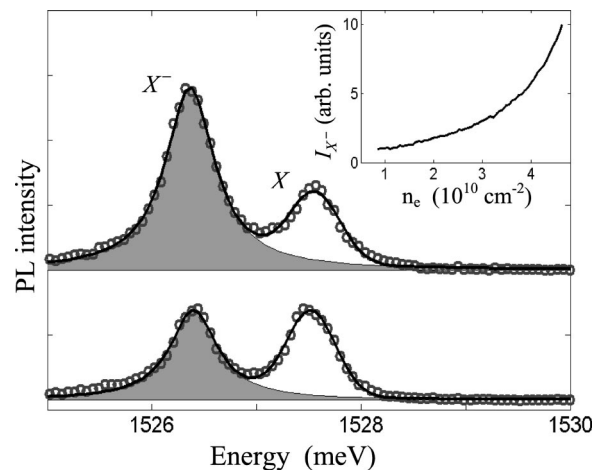


FIG. 1. PL spectra measured at two points, 0.5 μm apart. The peaks of the neutral exciton (X) and the negatively charged exciton (X^-) are marked in the figure. The solid line is a fit to the data points (circles). The X is fitted by a Gaussian and the X^- by a Lorentzian.¹¹ The shaded area is the integrated intensity. It is seen that the change in the X^- intensity is much larger than that of the X . Inset: The integrated X^- far-field intensity as a function of the average electron density n_e . Note the monotonic dependence of X^- intensity on n_e .

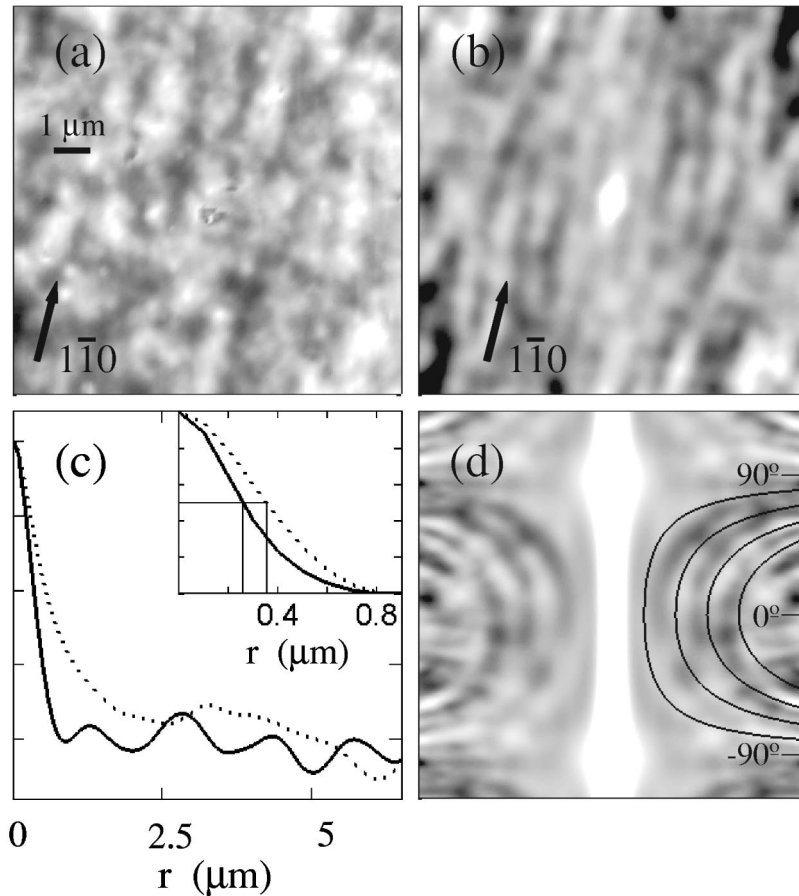


FIG. 2. (a) Two-dimensional image of the X^- integrated intensity, $I_{X^-}(x,y)$, in an area of $11 \times 11 \mu\text{m}^2$. The image is color-coded from dark to bright, corresponding to intensity changes by a factor of four. The arrow indicates the $[1\bar{1}0]$ crystal orientation. (b) The two-dimensional autocorrelation function $G(x,y)$ of $I_{X^-}(x,y)$ for the range $-8 \mu\text{m} \leq x,y \leq 8 \mu\text{m}$. Clear periodic electron density stripes are seen in the figure. (c) Two cuts through the origin of $G(x,y)$ along the $[1\bar{1}0]$ (dashed) and $[110]$ (solid) directions. Inset: The central peak of the cut along $[110]$ measured with tip diameters of $0.2 \mu\text{m}$ (solid) and $0.3 \mu\text{m}$ (dotted). The thin lines show the half width at half maximum. (d) The angular autocorrelation function $H(r,\theta)$ of $I_{X^-}(x,y)$. The function describes cuts through $G(x,y)$ at different angles θ . Clear concentric contours are observed, describing the gradual change of the periodicity with θ . The solid lines show the peaks of $H(r,\theta)$ for ideal periodic stripes, given by $r_n = n\lambda/\cos \theta$, with $\lambda = 1.3 \mu\text{m}$.

the 2DES with weak laser light and conducting a spatially resolved measurement of the PL spectrum, we can image the electron distribution in the plane.

The local measurement of the PL spectrum is realized using a homemade near-field scanning optical microscope¹² (NSOM) operating at 4.2 K. The sample is illuminated uniformly by a single-mode fiber, and the emitted PL is collected through a tapered Al-coated optical fiber tip, which is brought into close proximity ($< 10 \text{ nm}$) of the sample surface. The tip collects the PL and guides it through an optical fiber into a spectrometer, where it is dispersed onto a liquid-nitrogen-cooled charged-coupled-device (CCD) camera. The overall spectral resolution is $80 \mu\text{eV}$. The spatial resolution is determined by the tip diameter. We have conducted measurements with tips of various diameters, between 0.2 – $0.3 \mu\text{m}$. The two-dimensional images shown in this paper were

measured with a $0.3 \mu\text{m}$ tip, for which the higher collection efficiency allowed shortening of the acquisition time.¹³

The experiment is conducted on a 20 nm GaAs QW. A δ -doped donor layer with a density of $2.5 \times 10^{12} \text{ cm}^{-2}$ is separated from the QW by a 50 nm $\text{Al}_{0.36}\text{Ga}_{0.64}\text{As}$ spacer layer. The distance between the QW and the sample surface is 96 nm , and the total thickness of the MBE grown layers is $1.55 \mu\text{m}$. A $2 \times 2 \mu\text{m}^2$ mesa was etched, and Ohmic contacts were alloyed to the 2DES layer. A 4.5 nm PdAu semi-transparent gate was evaporated on top of the mesa. By applying a voltage between the gate and the 2DES, we could vary the electron density under illumination between 1×10^{10} and $2.5 \times 10^{11} \text{ cm}^{-2}$. The electron mobility exhibits anisotropy, being $3 \times 10^6 \text{ cm}^2/(\text{V sec})$ along the $[1\bar{1}0]$ direction and $2 \times 10^6 \text{ cm}^2/(\text{V sec})$ in the orthogonal direction.¹⁴

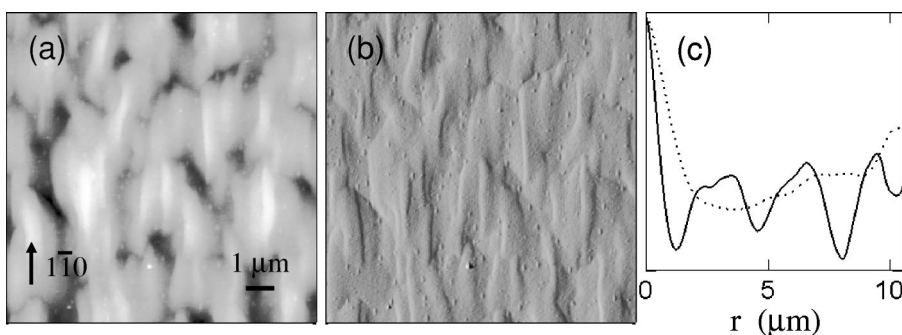


FIG. 3. (a) Typical AFM image of the crystal surface of an area of $11 \times 11 \mu\text{m}^2$. The vertical range is 20 nm . (b) The variations in cantilever amplitude which are proportional to the topography derivative. (c) Two cuts through the origin of the topography autocorrelation function along the $[1\bar{1}0]$ (dashed) and $[110]$ (solid) directions.

Figure 2(a) shows a two-dimensional image of $I_{X^-}(x,y)$, which is proportional to the electron density, in an area of $11 \times 11 \mu\text{m}^2$. The image shown here was measured at an electron density of $3 \times 10^{10} \text{ cm}^{-2}$. In this low density regime the fluctuations in the electron density are large compared to the average density, and hence, it is a convenient regime in which to measure them.³ Similar images have been measured at different gate voltages, in different regions of the same sample, and on different gated 2DES samples. It is seen that the 2DES density is highly nonuniform and exhibits large random fluctuations, manifested as changes of $I_{X^-}(x,y)$. The X intensity image (not shown), on the other hand, is very uniform and shows much smaller and more gradual fluctuations. This behavior is consistent with the fact that the neutral exciton can diffuse in the plane, and it provides reassuring evidence for the significance of the observed fluctuations.

To unveil possible order in this seemingly random image we have studied the X^- intensity autocorrelation function $G(x,y) = \langle I(x',y')I(x'-x,y'-y) \rangle$, where $\langle \rangle$ denotes averaging over all measured points in the scanned area, and $I(x,y)$ is the difference between $I_{X^-}(x,y)$ and its intensity average over all points, i.e., $I(x,y) = I_{X^-}(x,y) - \langle I_{X^-}(x,y) \rangle$. The correlation function averages out the random behavior and highlights the correlated part of the signal. The width of its central peak provides the correlation length, namely, the typical cluster size, and periodic peaks in $G(x,y)$ indicate the existence of periodicity in the electron distribution. The function $G(x,y)$ is shown in Fig. 2(b), with bright and dark colors signifying high and low correlation amplitude, respectively. It is seen that there is a pronounced anisotropy in $G(x,y)$: it is dominated by periodic stripes and its central peak is elongated parallel to $[1\bar{1}0]$. To better understand this behavior, we show in Fig. 2(c) two cuts through the origin of $G(x,y)$, one along $[1\bar{1}0]$ (dashed) and the other perpendicular to it, along $[110]$ (solid). We can see that both the short- and long-range correlations are different. The cut along the $[110]$ direction exhibits a correlation length of $0.35 \mu\text{m}$ (half-width at half maximum), and clear long-range oscillations with a periodicity of $\sim 1.3 \mu\text{m}$. The $[1\bar{1}0]$ cut, on the other hand, shows a significantly larger correlation length, $0.6 \mu\text{m}$, and no significant long-range order. We have verified that this behavior is not an instrument artifact by both rastering at different angles and by rotating the sample relative to the scan direction. Furthermore, no stripes were observed in the X intensity image. The correlation length along the $[110]$ direction, $0.35 \mu\text{m}$, is only slightly larger than the tip diameter, which is $0.3 \mu\text{m}$. In the inset of Fig. 2(c) we compare the central peak measured with tips having 0.2 and $0.3 \mu\text{m}$ diameters. The correlation length is seen to scale with the tip diameter, and it is $0.25 \mu\text{m}$ with the smaller tip. This allows us to determine the width of the stripes, after deconvolving the tip diameter, to be smaller than 150 nm .

The formation of electron density stripes is further emphasized by making cuts in $G(x,y)$ at different angles, θ . This is formally defined as the angular autocorrelation function $H(r,\theta) = \langle I(x',y')I(x'-r\cos\theta,y'-r\sin\theta) \rangle$. The re-

sults are shown in Fig. 2(d), with the horizontal scale being r and the vertical scale being θ . Clear concentric contours are observed, describing a gradual change of the periodicity with θ . It is easy to see that this behavior indeed corresponds to periodic electron density stripes along the $[1\bar{1}0]$ direction. Clearly, the oscillation period of such a stripe pattern would vary with θ as $\lambda/\cos\theta$, where λ is the period of the stripes.

The fact that the electron density stripes coincide with crystalline orientation and the relatively large periodicity, points to an underlying crystalline structure as the source of this behavior. To examine this possibility we performed atomic force microscopy (AFM) measurements of the crystal surface on different pieces of the same wafer. Figure 3(a) shows a typical topography image and Fig. 3(b) shows the variations in cantilever amplitude, which are proportional to the topography derivative. It is seen that narrow ridges, which are oriented along the $[1\bar{1}0]$ direction, cover the sample surface. The formation of these ridges is well studied and understood. Their origin is an intrinsic growth instability, which inhibits downward movement of adatoms at surface step edges, and leads to the buildup of mounds.¹⁵ The heights of these mounds and their typical size increase with the number of layers grown,¹⁶ and their anisotropy is due to the particular surface reconstruction of the As atoms that terminate the (001) surface.¹⁷ The dangling bonds of these atoms form dimers that are arranged in rows along the $[1\bar{1}0]$ direction, and since the growth rate along the dimer rows is larger than in the orthogonal direction, the mounds become elongated along $[1\bar{1}0]$. Clearly, these mounds modulate the distances of the ionized donors layer and the crystal surface relative to the 2DES plane, and thereby cause variations in the electrostatic potential in that plane. Considering the structure as a parallel plate capacitor (gate and 2DES) with a positively charged layer (the donors) in between, it is straightforward to show that varying the distances of these layers in our sample by a monolayer would be translated to a density change of $\sim 10^9 \text{ cm}^{-2}$ in the 2DES.

The relation between the density distribution and the crystal topography is best demonstrated by comparing the autocorrelation functions of the density distribution and that of the topography image. Figure 3(c) shows two cuts of the topography autocorrelation function along $[1\bar{1}0]$ (dashed) and $[110]$ (solid). The similarity between Figs. 2(c) and 3(c) is evident. We notice, however, that the periodicity in the topography image is considerably larger than that of the electron density stripes. This larger period was found in all AFM measurements of different areas of the same wafer. The difference between the surface mounds and the electron density periods is not surprising. The coarsening process that occurs during the growth, in which small mounds join to form larger ones, results in an increase of the period towards the surface. Hence, the distance between the 2DES and the surface would be modulated with a period, which is roughly the average between the mounds period at the surface and at the 2DES.

It should be emphasized that other disorder potentials might also affect the electron distribution. Fluctuations in the QW width cause the electron confinement energy in the well to vary from one point to another and hence introduce po-

tential fluctuations. These fluctuations can be imaged as well in our experiment by determining the X peak energy at each point.^{2,4} We have found that the well width fluctuations, despite being sensitive to the mounds,¹⁸ show no correlation with the charge fluctuations. The QW width fluctuations, as well as the fluctuations in the donor density, are the probable source of the random density pattern, which is evident in Fig. 2(a) but averages out in the correlation function.

It is interesting to consider our results in the context of the recent debate on the origin of transport anisotropy in high Landau levels.^{19–21} Our observation of charge stripes provides direct support for the suggestion that the transport anisotropy is due to the underlying crystalline structure.²⁰ Finally, we wish to note that the elongated mounds are an

intrinsic property of MBE growth and are found even in the highest mobility samples.^{20,21} Hence, the electron density stripes formation is a fundamental property of 2DES systems, and should play a particularly important role at low electron densities, where the electrons form a network of quasi-one-dimensional wires.

We are pleased to acknowledge D. Kandel for helpful discussions on the MBE growth, E. Khivrich for his assistance in the AFM measurements, and G. Fish from Nanonics for providing the NSOM tips.

The research was partially supported by the Israeli Science Foundation and the Minerva Foundation.

¹H. L. Stormer *et al.*, Appl. Phys. Lett. **38**, 691 (1981).

²H. F. Hess *et al.*, Science **264**, 1740 (1994).

³G. Eytan *et al.*, Phys. Rev. Lett. **81**, 1666 (1998).

⁴Q. Wu *et al.*, Phys. Rev. Lett. **83**, 2652 (1999).

⁵S. H. Tessmer *et al.*, Nature (London) **392**, 51 (1998).

⁶A. Yacoby *et al.*, Solid State Commun. **111**, 1 (1999).

⁷E. Betzig and J. K. Trautman, Science **257**, 189 (1992).

⁸M. A. Paelser and P. J. Moyer, *Near Field Optics* (Wiley, New York, 1996).

⁹K. Kheng *et al.*, Phys. Rev. Lett. **71**, 1752 (1993).

¹⁰G. Finkelstein, H. Shtrikman, and I. Bar-Joseph, Phys. Rev. Lett. **74**, 976 (1995).

¹¹Y. Yayan *et al.*, Phys. Rev. B **64**, 081308 (2001).

¹²G. Eytan *et al.*, Ultramicroscopy **83**, 25 (2000).

¹³The tip size was determined by measuring the PL from local defects.

¹⁴The determination of the $[1\bar{1}0]$ direction was done by identifying the “bowtie” defects on the back of the sample.

¹⁵M. D. Johnson *et al.*, Phys. Rev. Lett. **72**, 116 (1994).

¹⁶C. Orme *et al.*, Appl. Phys. Lett. **64**, 860 (1994).

¹⁷The arsenic overpressure causes the crystal surface to be terminated by arsenic atoms.

¹⁸The behavior of the well width fluctuations will be reported elsewhere.

¹⁹M. P. Lilly *et al.*, Phys. Rev. Lett. **82**, 394 (1999).

²⁰K. B. Cooper *et al.*, Solid State Commun. **119**, 89 (2001).

²¹R. L. Willett *et al.*, Phys. Rev. Lett. **87**, 126803 (2001).